The Astrophysical Journal, 619:884–890, 2005 February 1

FAR ULTRAVIOLET SPECTROSCOPIC EXPLORER MEASUREMENTS OF INTERSTELLAR FLUORINE[1]

S. R. Federman,[2] Yaron Sheffer,[2] David L. Lambert,[3] and V. V. Smith[4]

Received 2004 May 3; accepted 2004 October 14

ABSTRACT

The source of fluorine is not well understood, although core-collapse supernovae, Wolf-Rayet stars, and asymptotic giant branch stars have been suggested. A search for evidence of the ν-process during Type II supernovae is presented. Absorption from interstellar F I is seen in spectra of HD 208440 and HD 209339A acquired with the *Far Ultraviolet Spectroscopic Explorer*. In order to extract the column density for F I from the line at 954 Å, absorption from H_2 has to be modeled and then removed. Our analysis indicates that for H_2 column densities less than about 3×10^{20} cm^{-2}, the amount of F I can be determined from λ954. For these two sight lines, there is no clear indication for enhanced F abundances resulting from the ν-process in a region shaped by past supernovae.

Subject headings: ISM: abundances — ISM: atoms — nuclear reactions, nucleosynthesis, abundances — stars: individual (HD 208440, HD 209339A)

1. INTRODUCTION

While fluorine consists of the single stable isotope ^{19}F, theories of stellar nucleosynthesis have not yet been able to clearly identify the origin of this element. Three astrophysical sites are currently suggested as possible significant sources: core-collapse supernovae (SNe II), Wolf-Rayet stars, and asymptotic giant branch (AGB) stars. In SNe II, the enormous flux of neutrinos escaping the core interact with ^{20}Ne in the Ne shell, causing evaporation of a proton or neutron and (in both cases) conversion of a small amount of ^{20}Ne to ^{19}F (Woosley et al. 1990). This neutrino nucleosynthesis is often called the "ν-process." In Wolf-Rayet stars, ^{19}F is produced inside the star mainly at the beginning of the He-burning phase; this fluorine will be destroyed later in the evolution of the star unless extensive mass loss removes the star's layers down to the regions where ^{19}F has been synthesized and then ejected into space (Meynet & Arnould 2000). For AGB stars, Jorissen et al. (1992) suggested that ^{19}F is a by-product of neutron captures during He burning; Mowlavi et al. (1998) provided a detailed description of the process. In our effort to understand the source of fluorine, we present the first measurements of interstellar F with the *Far Ultraviolet Spectroscopic Explorer* (*FUSE*) via absorption from F I λ954.

There are very few observations of F outside the solar system. Observations of HF via rotational-vibrational lines in the infrared (Jorissen et al. 1992) are limited to the coolest giants. More recently, Cunha et al. (2003) measured HF absorption from red giants in the Large Magellanic Cloud and ω Cen. They found that the F/O abundance ratio declined as the O abundance declined, a trend expected for ν-process synthesis of F, but Wolf-Rayet stars remain a possibility. Liu (1998) obtained the only definitive fluorine abundance in a planetary nebula (NGC 4361) via [F IV] λ4060. Interstellar F I was detected through the line at 954 Å toward δ Sco by Snow & York (1981), who used the *Copernicus* satellite; the measured equivalent width of $10.9^{+4.5}_{-3.1}$ mÅ translates into an abundance, $\log \epsilon(\mathrm{F}) = \log(\mathrm{F/H}) + 12$, of ~ 4.0. The solar system abundance is 4.48 ± 0.06 from meteorites and 4.60 ± 0.30 from HF lines in sunspots (Anders & Grevesse 1989). Neufeld et al. (1997) detected HF absorption at 121.7 μm with the Infrared Space Observatory (*ISO*) satellite from interstellar gas in Sgr B2, a giant molecular cloud near the Galactic center. Chemical models (see also Zhu et al. 2002) indicate that most of the fluorine in molecular clouds should be in HF, while analysis of HF excitation suggests severe fluorine depletion assuming the solar system abundance is the appropriate measure for comparison. The results on the abundance of interstellar F from HF are consistent with those for HCl in this cloud (Zmuidzinas et al. 1995), another hydrogen halide. However, the apparent extreme levels of depletion for both species and the unknown reference for elemental abundances in the vicinity of the Galactic center make it hard to interpret these results from a cosmochemical perspective. Of the suite of observations, only those of Jorissen et al. (1992) provide clear evidence for a site of F production: thermally pulsing AGB stars that also make *s*-process nuclides.

This paper describes the detection of F I absorption toward HD 208440 and HD 209339A, which are about 900 pc from the Sun (e.g., Pan et al. 2004). These stars were chosen for study because they belong to the Cepheus OB2 association, an ideal site to search for ν-process products. The stars in Cep OB2 formed in an expanding shell of gas created by previous members of the cluster NGC 7160 when their lives ended in SNe II (Patel et al. 1995, 1998). Absorption from H_2 is also present at 954 Å and must be removed for an accurate measurement of F I; our analysis provides a limiting H_2 column density for new F I λ954 searches. The focus of our interpretation is on abundance ratios because elemental abundances are less accurately known, a result of the relatively large uncertainties in total hydrogen column densities. In particular, we examine F/Cl, N/O, and F/O ratios. Column densities for Cl I, Cl II, and N I come from *FUSE* spectra, while absorption from O I and another strong line of Cl I comes from data acquired with the Space Telescope Imaging Spectrograph (STIS) on the *Hubble Space Telescope* (*HST*). The F/Cl ratio is useful in ascertaining the presence of an anomalous F abundance because both halogens are expected to have similar

[1] Based on observations made with the NASA/CNES/CSA *Far Ultraviolet Spectroscopic Explorer* (*FUSE*), which is operated for NASA by the Johns Hopkins University under NASA contract NAS 5-32985.

[2] Department of Physics and Astronomy, University of Toledo, Toledo, OH 43606; steven.federman@utoledo.edu; ysheffer@physics.utoledo.edu.

[3] W. J. McDonald Observatory, University of Texas, Austin, TX 78712; dll@astro.as.utexas.edu.

[4] Department of Physics, University of Texas at El Paso, El Paso, TX 79968; verne@barium.physics.utep.edu.

levels of depletion onto interstellar grains. The ratio of two volatile elements, N and O, is useful for probing the overall level of depletion. With the information gleaned from the F/Cl and N/O ratios, we can explore what the F/O ratios say about the site of F nucleosynthesis.

2. OBSERVATIONS

2.1. *FUSE Measurements*

The stars, HD 208440 and HD 209339A, were observed by *FUSE* for program B030. As the two brightest among five target stars, they offered better spectra with higher signal-to-noise (S/N) ratios. They also have lower H_2 column density and therefore higher residual signal at the position of the F I line at 954 Å. The observations on HD 208440 took place on 2001 August 3 during three orbits with a total exposure time of 9777 s in 15 subexposures. The data for HD 209339A were acquired on 2002 July 21 during a single orbit with a total exposure time of 2044 s divided into four subexposures. Both stars were observed in histogram (HIST) mode through the low-resolution aperture. The data were processed with CALFUSE version 2.4. We then rebinned the data by a factor of 4, yielding an S/N of ~30 at 950 Å and a two-pixel resolution element of about 0.06 Å, with respective resolving powers of ~17,500 and ~15,000 for the LiF and SiC segments, respectively.

In addition to the F I line at 954 Å, the *FUSE* spectra included other lines of use for our analysis. The weaker F I line at 951 Å, although not detected, provided a check on the column density derived from λ954. The $B - X$ 2–0, 3–0, and 4–0 Lyman bands of H_2 between 1042 and 1083 Å were used to infer the H_2 column density; this column density allowed us to remove the H_2 absorption in the vicinity of 954 Å. Cl I $\lambda\lambda$1088, 1097 and Cl II λ1071 yielded the total amount of Cl along the line of sight. Since the Cl I line at 1088 Å is partially blended with the $C - X$ 0–0 band of CO, we had to determine the CO column density as well. This was accomplished by a simultaneous fit to the $C - X$ 0–0 and $E - X$ 0–0 bands seen in *FUSE* spectra and to $A - X$ bands in STIS spectra. Finally, the (relatively) weak N I line at 1160 Å provided the nitrogen column density.

2.2. *HST Observations*

We also used archival spectra of the two stars from *HST*/STIS observations. For HD 208440, the available spectrum (data set O5LH0B) was taken through the $0\farcs2 \times 0\farcs2$ slit at $R = 110{,}000$, while the HD 209339A data (from O5C06M) were secured with the highest resolution slit ($0\farcs1 \times 0\farcs025$) that provided $R \sim 200{,}000$. Pixels, not subpixels, were adopted for the spectrum of HD 209339A, thereby giving us a higher S/N and a spectral resolution like that for HD 208440. These STIS spectra were needed for our analysis of the weak O I line at 1355 Å, as well as the strong Cl I line at 1347 Å and the $A - X$ bands of CO.

3. ANALYSIS AND RESULTS

3.1. *Component Structure*

Since the ultraviolet measurements lacked the necessary spectral resolution to discern individual velocity components, the basis for the component structure was high-resolution ($R \approx 200{,}000$) ground-based measurements (Pan et al. 2004). In particular, we adopted the structure from CH λ4300 for our synthesis of the H_2 bands. For the atomic species, we used the velocity components showing absorption from K I λ7699 and the structure seen in Ca II K (3933 Å) for these components. In particular, the *b*-values, which essentially are a measure of the turbulent broadening for these species, and relative column densities of the Ca II lines formed the basis for synthesizing the atomic spectra. The Ca II structure was adopted for our syntheses of all atomic profiles because the species analyzed here are likely to be distributed more widely along the line of sight than is K I. Like Ca II, O I, N I, and F I are the dominant ions in neutral diffuse clouds, while Cl I probably represents an intermediate situation. Inclusion of the additional components seen in the Ca II K spectrum did not improve the fits.

3.2. *Profile Synthesis*

The features of interest in the *FUSE* spectra covered most of the spectral passband. For the determination of the H_2 column density from the Lyman bands, we used three of the four overlapping segments LiF-1A, SiC-1A, and SiC-2B. The spectra from LiF-2B were included in the analysis only when the results were not significantly different. The F I lines were covered by segments SiC-2A and SiC-1B, and the N I line at 1160 Å was present in segments LiF-2A and LiF-1B. We co-added data from different segments to improve the S/N; no evidence for degradation of spectra was noticed over the short wavelength ranges of interest to us. For H_2, uncertainties were inferred from the range of results for individual segments. For the atomic lines, the uncertainties were based on uncertainties associated with equivalent widths and were determined from line width and rms dispersion about the continuum level. Our fits were performed with the code ISMOD, which uses simple rms-minimizing steps in parameter space to reach a desired level of acceptable fit, usually down to 10^{-4} in parameter relative values.

Our modeling of H_2 was based on a line list maintained by S. R. McCandliss.[5] The normalized continuum was determined by a linear fit of the highest spectral regions for a given segment. The column density of H_2 is not especially sensitive to the cloud structure for our sight lines because it is derived from damping wings of the $J = 0$ and $J = 1$ lines, the two levels containing most of the H_2 column density. We made sure that the H_2 model does not go below the observed flux, i.e., we avoided creating "emission" residuals. In contrast, the stellar flux tends to dip below the fitted H_2 profile owing to the presence of stellar absorption lines that were not synthesized. These lines, however, are exponentially extinguished by H_2 absorption so that for regions of very low residual intensity, the fitted H_2 profile and the data tend to agree extremely well—see Figure 1. In spectral regions with relatively weak attenuation by H_2, we eliminated the undulations from stellar absorption lines by rectifying the continuum over a short interval up to 1 Å away from interstellar lines of interest with low-order polynomials.

We used the fact that H_2 and CH track each other well (Federman 1982; Danks et al. 1984) in synthesizing the Lyman bands. There are four and two CH components toward HD 208440 and HD 209339A, respectively. The relative velocities and fractions were held fixed in our syntheses, but we modified the *b*-values of the components to take into account the different masses of H_2 and CH. This can only be accomplished once the kinetic temperature ($T_{\rm kin}$) is known; thus *b*-values were fitted along with the rotational excitation temperature from the relative populations of the $J = 1$ and 0 levels of H_2, $T_{1,0}$. Such a procedure is based on the usual assumption that $T_{1,0}$ is a fair representation of $T_{\rm kin}$. The final *b*-value for H_2 is a composite of the thermal width and the turbulent width; the latter produces most of the broadening in CH. In all, the free-fit parameters are

[5] Available at http://www.pha.jhu.edu/~stephan/H2ools/h1h2data/highjsh2vpnvpp0.dat.

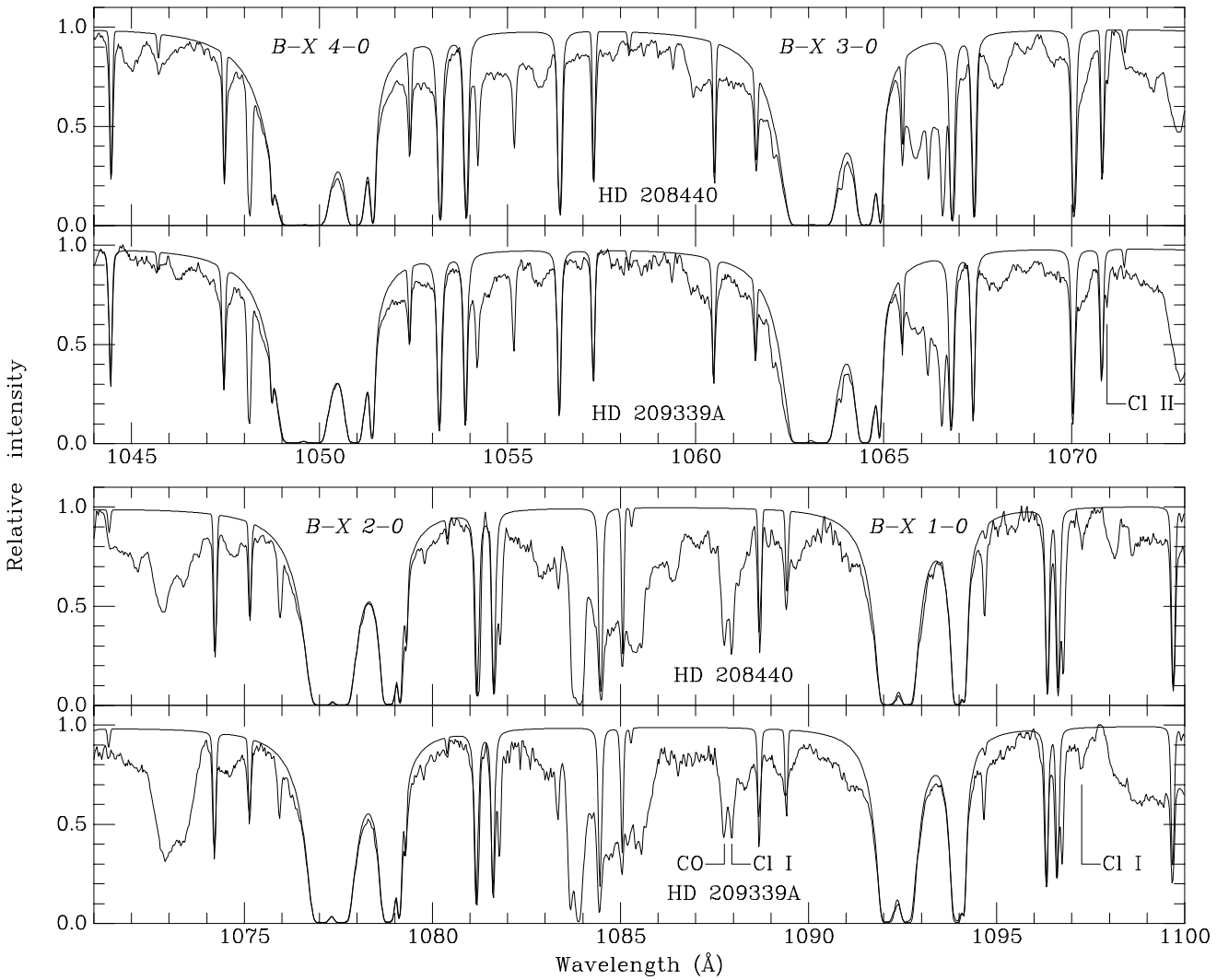

FIG. 1.—Global view of four H_2 Lyman bands toward HD 208440 (*first and third panels, top to bottom*) and HD 209339A (*second and fourth panels*). It is composed of LiF-1A data between 1041 and 1082 Å, of SiC-1A and SiC-2B data between 1082 and 1087 Å, and of LiF-2A data between 1087 and 1100 Å. The smooth curve shows the adopted H_2 model. It is based on a simultaneous fit of the 2–0, 3–0, and 4–0 bands for four *FUSE* segments (see text). This model yielded the excellent match for the 1–0 band near 1095 Å. Stellar features and other interstellar lines account for the rest of the absorption in the spectrum. The Cl I and Cl II lines as well as the CO $C - X$ band are indicated in the spectrum for HD 209339A.

total column density, $N(H_2)$, radial velocity of H_2, and six rotational excitation temperatures relative to the ground level, $T_{J'',0}$. The results of the syntheses for the component structures and for the column densities appear in Tables 1 and 2, respectively. For completeness, the b-value derived for H_2 and turbulent velocity, $v_{\rm turb}$, inferred from $b(H_2)$ and $T_{1,0}$ are also listed in Table 1. Since the sound speed for gas at 80 K that is mostly atomic is $\approx$1.2 km s^{-1}, the turbulent motions appear to be essentially sonic. (Further discussion of the results on H_2 and CO will be presented elsewhere [K. Pan et al. 2005, in preparation].)

TABLE 1
COMPONENT STRUCTURE FOR H_2 SYNTHESES

Parameter	HD 208440			HD 209339A		
$v_{\rm LSR}$[a] (km s^{-1}).....	−11.3	−8.2	−5.3	+1.0	−5.1	−2.3
Fraction[a] (%).....	0.30	0.14	0.33	0.23	0.39	0.61
b(CH)[a] (km s^{-1})....	1.3	1.0	1.4	1.3	0.9	1.0
$b(H_2)$(km s^{-1}).....	1.5	1.2	1.6	1.5	1.2	1.3
$v_{\rm turb}$[b] (km s^{-1})	1.3	0.9	1.4	1.3	0.8	1.0

[a] CH component structure from Pan et al. (2004).
[b] Obtained from $b(H_2)$ and $T_{1,0}$ of 76 and 91 K for HD 208440 and HD 209339A, respectively.

TABLE 2
RESULTS FOR H_2

	log $N(H_2)$	
J''	HD 208440	HD 209339A
0.....	20.04 ± 0.01	19.87 ± 0.01
1.....	20.02 ± 0.01	20.01 ± 0.01
2.....	18.41 ± 0.02	18.35 ± 0.04
3.....	18.12 ± 0.12	18.02 ± 0.07
4.....	16.03 ± 0.18	17.41 ± 0.05
5.....	15.09 ± 0.04	16.47 ± 0.21
6.....	14.24 ± 0.10	14.06 ± 0.06
Total	20.34 ± 0.01	20.25 ± 0.01

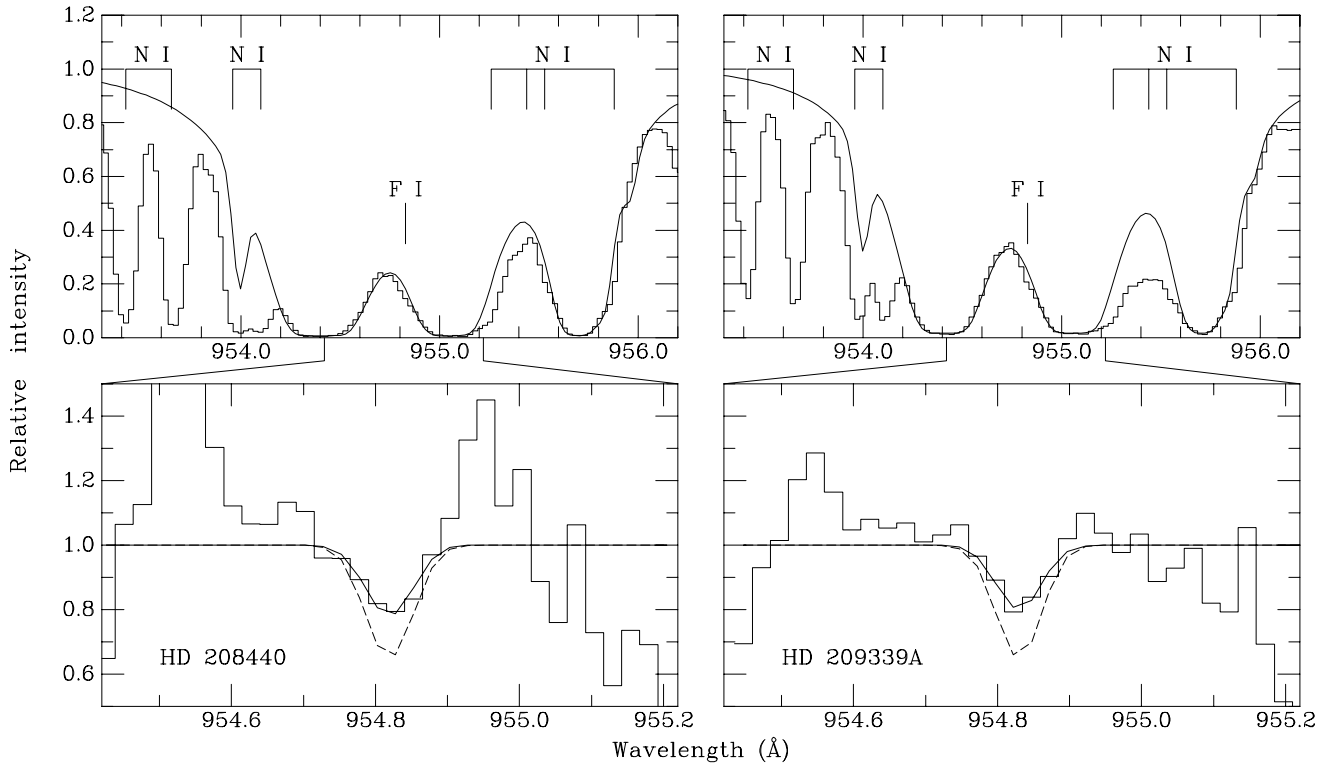

FIG. 2.—Spectra showing the steps leading to a determination for N(F I) toward HD 208440 (*left panels*) and HD 209339A (*right panels*). *Top panels*: Application of the H_2 model from Fig. 1 for lines blended with F I λ954. The N I lines, which were not fitted because they have substantial optical depths at line center but show no damping wings, account for the remaining absorption. *Bottom panels*: An expanded view showing the F I line upon removal of H_2 via division, resulting in strong residuals at H_2 line cores. The solid curve indicates the absorption associated with the column density given in Table 3, and the dashed curve indicates the expected absorption for the solar system abundance.

The next step in our analysis was extracting the column density of F I from the line at 954 Å. (The line at 951 Å, which is affected by the presence of H_2 absorption to a lesser degree, is too weak for detection in many sight lines, including the ones studied here.) Upon application of the H_2 results in Tables 1 and 2 to the H_2 lines in the vicinity of 954 Å, we saw excess absorption, which we attribute to F I. The model for the H_2 lines was divided into the spectrum, revealing the presence of λ954 more clearly. The F I absorption was fitted to our template for the atomic lines from measurements on K I and Ca II. Figure 2 illustrates the steps yielding an estimate of N(F I) for the gas toward HD 208440 and HD 209339A. Since both sight lines have $N(H_2)$ of about 2×10^{20} cm^{-2}, a limiting column density of 3×10^{20} cm^{-2}, when H_2 absorption becomes black and F I λ954 can no longer be detected, can be inferred from our spectra.

It should be emphasized that the H_2 model is very robust, thanks to its dominance over almost the entire *FUSE* spectral range, and that around the F I line, the continuum is formed by gently varying slopes from the wings of the $J = 0$ and 1 lines of H_2. Therefore, the actual curvature of the continuum on both sides of the 954 Å line is also very robust. In fact, we use the H_2 template to rectify the continuum, instead of applying an arbitrary polynomial within the IRAF/SPLOT task. This assures a much better match with the actual data. The only variables still affecting the placement of the H_2 model are the position on the wavelength scale and the alignment of the continuum level. We found that we needed to raise the continuum level of the H_2 template by 5% in order to avoid generating "emission" regions. This fact reflects the uncertainty involved with the original rectification over the *FUSE* segment. Because we divided by the H_2 profile, large noise spikes are generated whenever the residual intensity is very near zero, much larger, in fact, than the noise appropriate to the precise location of the F I line. The uncertainties in W_λ, therefore, were inferred from regions beyond the H_2 lines. Some excessive noise is apparent next to the F I line in HD 208440, in which the cores of the H_2 lines seem to be narrower than their templates. This could be caused by extra noise in this spectrum, perhaps because HD 208440 has lower flux levels than those of HD 209339A. Indeed, the *FUSE* exposure time was longer toward HD 208440, but not by a sufficiently large factor to fully compensate for the lower flux levels.

Despite the noisy conditions after division by H_2 line cores, there is good signal for the 954 Å line in both stars, with $W_\lambda \geq$ 15 mÅ. The line is present in the individual segments SiC-2A and SiC-1B prior to their co-addition. Therefore, there is no doubt that the detection is real, since it is independent of the segment being used, of pixel position, and of the line of sight being probed. The only issue that has to be settled is whether the observed lines might be stellar in origin, rather than being interstellar. These lines are indeed interstellar because their radial velocity agrees very well (within 2 km s^{-1}) with that of the H_2 lines and because their width is as narrow as the other interstellar lines, while stellar lines are appreciably wider. In fact, as can be seen in Figure 2, the fit of the interstellar cloud structure to the observed widths is very good.

As noted above, an important ingredient of our analysis is knowledge of the total chlorine column density, N(Cl I) + N(Cl II). For Cl I, the line at 1097 Å is rather weak, while λ1347 is quite strong. The line at 1088 Å is intermediate in strength and therefore apparently very useful, but it is blended with a CO band.

TABLE 3
Atomic Results

Species	λ (Å)	f-value	HD 208440 W_λ (mÅ)	HD 208440 N (cm^{-2})	HD 209339A W_λ (mÅ)	HD 209339A N (cm^{-2})
F I	954.8	8.17×10^{-2}[a]	18 ± 7	$(3.3\pm1.5)\times10^{13}$	16 ± 6	$(2.9\pm1.4)\times10^{13}$
Cl II	1071.0	1.50×10^{-2}[a]	23.0 ± 1.4	$(1.9\pm0.1)\times10^{14}$	17.3 ± 1.2	$(1.4\pm0.1)\times10^{14}$
Cl I	1088.0	8.10×10^{-2}[b]	46.1 ± 1.4	$(9.0\pm0.5)\times10^{13}$[c]	38 ± 3	$(8.5\pm1.0)\times10^{13}$[c]
	1097.4	8.80×10^{-3}[b]	7.5 ± 0.7	$(8.5\pm0.8)\times10^{13}$[c]	8.8 ± 0.5	$(9.1\pm0.6)\times10^{13}$[c]
	1347.2	1.53×10^{-1}[b]	88.8 ± 0.8	$(14.4\pm0.9)\times10^{13}$[c]	74.2 ± 0.5	$(9.8\pm0.3)\times10^{13}$[c]
N I	1159.8	9.95×10^{-6}[a]	16.2 ± 0.8	$(1.55\pm0.08)\times10^{17}$	15.0 ± 0.6	$(1.46\pm0.06)\times10^{17}$
O I	1355.6	1.16×10^{-6}[a]	15.1 ± 0.9	$(8.8\pm0.5)\times10^{17}$	16.4 ± 0.4	$(9.9\pm0.2)\times10^{17}$

[a] Oscillator strengths from Morton (2003).
[b] Oscillator strengths for Cl I from Schectman et al. (1993).
[c] An unweighted average yields N(Cl I) of $(10.6\pm3.3)\times10^{13}$ and $(9.1\pm1.6)\times10^{13}$ cm^{-2} toward HD 208440 and HD 209339A, respectively.

By synthesizing the CO bands in our *FUSE* and STIS spectra with the component structure from CH, we were able to incorporate λ1088 into our determination for N(Cl I). The synthesis of the CO bands was done in two parts: fitting the observations of the $A-X$ and $E-X$ bands and then including the stronger $C-X$ band in the model for CO absorption. Our values for N(CO) are $(1.60\pm0.06)\times10^{14}$ and $(9.2\pm1.0)\times10^{13}$ cm^{-2} for the clouds toward HD 208440 and HD 209339A, respectively. The resulting column densities for the chlorine ions and the other atoms are listed in Table 3. These column densities are based on fits with seven velocity components toward both stars. Only the velocity zero point was allowed to vary in the syntheses of atomic profiles; the residuals from these fits are indistinguishable from the fluctuations in the continuum on either side of the profile. The atomic spectra appear in Figures 3 and 4.

4. DISCUSSION

The column densities in Table 3 were used for the elemental abundance ratios displayed in Table 4, which includes ratios for the gas toward δ Sco and for the solar system for comparison. For

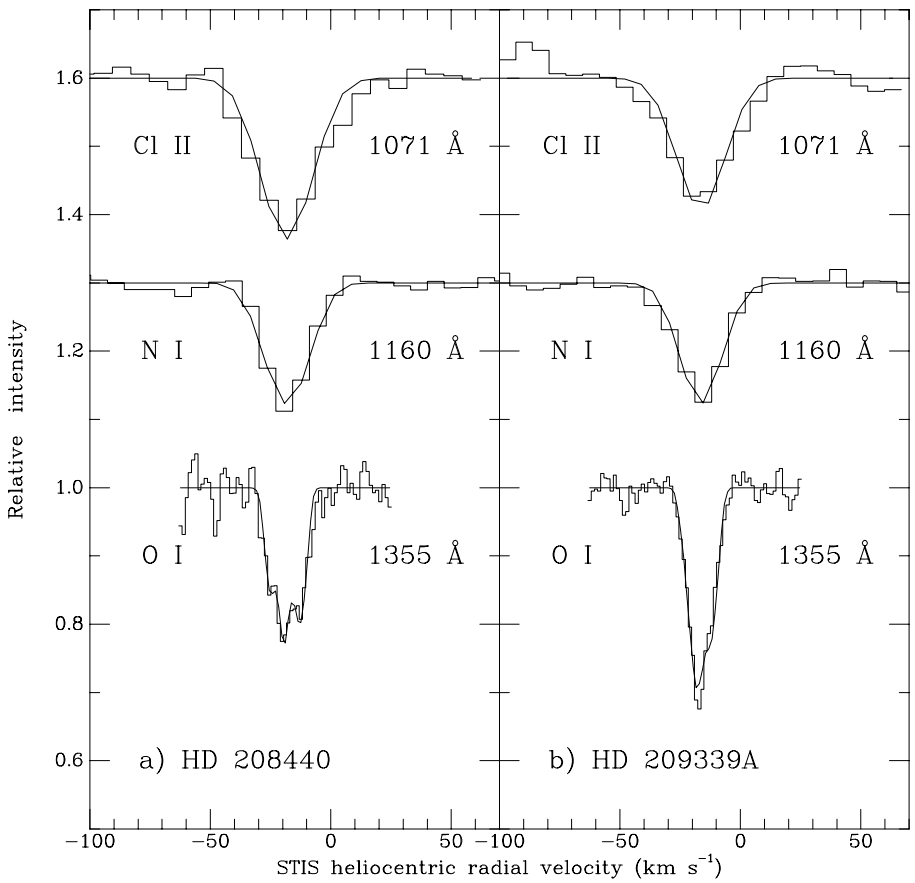

Fig. 3.—Interstellar absorption from Cl II (offset to 1.6), N I (offset to 1.3), and O I toward (*a*) HD 208440 and (*b*) HD 209339A (*histograms*), with the results from Table 3 presented as smooth curves. Note the higher resolution of STIS spectra relative to *FUSE* data. The latter were aligned with the radial velocity of the STIS observation.

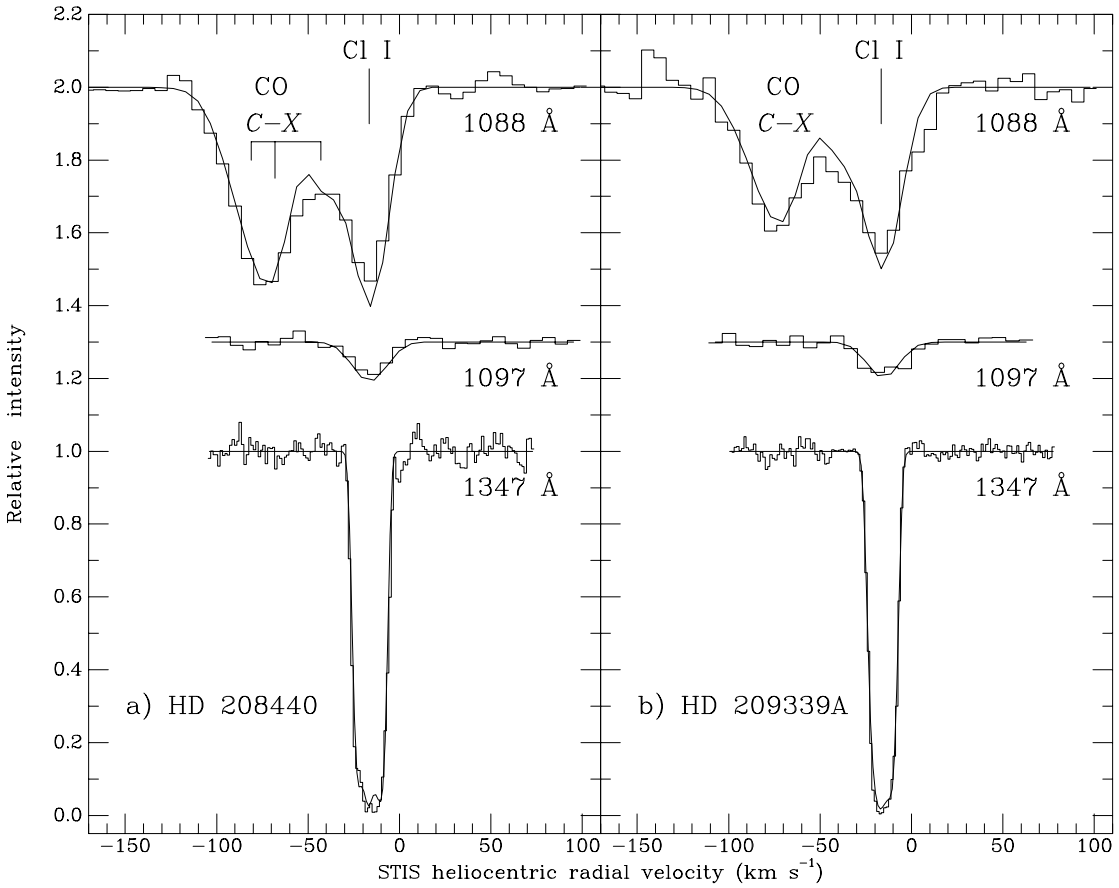

FIG. 4.—Interstellar absorption from three lines of Cl I toward (*a*) HD 208440 and (*b*) HD 209339A. The spectra for λ1097 and λ1088 are shifted upward by 0.3 and 1.0, respectively, for clarity. The average results are indicated by the fits. The strong λ1347 line is from STIS spectra. The λ1088 line from *FUSE* is blended with the $C - X$ 0–0 band of CO. The positions of the $R(1)$, $R(0)$, and $P(1)$ lines of CO are shown in the HD 208440 panel. All lines up to $J = 5$ for four CO bands, together with Cl I λ1088, were fitted simultaneously. For the $C - X$ band toward HD 209339A, only SiC segments were used.

δ Sco, values of W_λ were obtained from the literature (Snow & York 1981 for F I; Bohlin et al. 1983 for Cl II and Cl I λ1097; Meyer et al. 1997 for N I; Meyer et al. 1998 for O I) and were converted into column densities through a curve-of-growth analysis with a *b*-value of 2.5 km s^{-1} for the main K I component (Welty & Hobbs 2001). The adopted *b*-value is consistent with the value inferred for dominant ions in the main cloud toward ζ Oph (Savage et al. 1992). For the solar system ratios, we used the results quoted by Anders & Grevesse (1989) and Grevesse & Sauval (1998) for N, F, and Cl and the newly revised solar O abundance (Allende Prieto et al. 2001). Since N I, O I, and F I represent the dominant ions in relatively dense, neutral diffuse clouds probed by our observations, and Cl I and Cl II represent essentially all the Cl, we do not include the ion stage in what follows.

We first consider the F/Cl and N/O ratios, which are measures of unusual atomic abundances. The three interstellar values for F/Cl in diffuse clouds are indistinguishable from the meteoritic value (0.16) at the 1 σ level. This is not surprising, since both halogens are expected to have similar solid-state chemical behaviors. The interstellar values for N/O are also consistent with the ratio of 0.17 found in the solar photosphere, as well as the value (0.18 ± 0.02) obtained from interstellar surveys on N (Meyer et al. 1997) and O (Cartledge et al. 2001) with a common set of *f*-values. Moreover, a relatively accurate column density for atomic hydrogen (Diplas & Savage 1994) allows us to derive the elemental O abundance, $N(\mathrm{O})/[N(\mathrm{H\,I}) + 2N(\mathrm{H_2})]$, toward HD 208440; the result is $(4.2 \pm 0.8) \times 10^{-4}$, compared to the average interstellar value of $(3.47 \pm 0.16) \times 10^{-4}$ (Cartledge et al. 2001). A recent independent analysis for this star (Cartledge et al. 2004) yielded $(4.4 \pm 1.1) \times 10^{-4}$. Since the lines of sight toward HD 208440 and HD 209339A have similar O and H_2 column densities and similar amounts of reddening (0.34 vs. 0.37), we infer that these sight lines do not have enhanced depletion of O onto grains.

As seen in Table 4, the interstellar results for F/O are compatible with each other, but their weighted mean of $(3.4 \pm 1.0) \times 10^{-5}$ is about half the solar system ratio. The bottom panels in

TABLE 4
OBSERVED ELEMENTAL ABUNDANCE RATIOS

Ratio	HD 208440	HD 209339A	δ Sco	Solar System
F/Cl.....	0.11 ± 0.06	0.12 ± 0.06	0.17 ± 0.10	0.16 ± 0.03
N/O.....	0.18 ± 0.01	0.15 ± 0.01	0.21 ± 0.02	0.17 ± 0.03
F/O ($\times 10^{-5}$)	3.8 ± 1.7	2.9 ± 1.4	3.9 ± 2.2	6.1 ± 1.2

Figure 2 illustrate this fact by revealing how a column density for F I based on the solar system abundance for F is not consistent with the data for λ954. This suggests that the sight lines have somewhat more F (and Cl) depletion compared with the depletion levels for O (and N). The most recent compilation of solar system abundances (Lodders 2003) lists meteoritic results for F and Cl that are 0.02 dex (5%) lower than the values adopted here (although within the uncertainties for both determinations). Such a small difference does not affect our conclusions.

When the levels of depletion for Li and K (e.g., Knauth et al. 2003), two other elements forming relatively volatile compounds, are added to our results for N, O, F, and Cl, a trend with condensation temperature ($T_{\rm cond}$) emerges. (The comparison is based on the condensation temperatures quoted by Lodders [2003].) Relative to solar system abundances, N and O ($T_{\rm cond} \sim$ 150 K) are depleted by a factor of about 30%, F and Cl ($T_{\rm cond} \sim$ 800 K) by a factor of 45%, and Li and K ($T_{\rm cond} = 1000$–1100 K) by a factor of 85%.

There is no clear indication of enhanced F abundances resulting from the ν-process in SNe II, although the Cep OB2 association experienced core-collapse supernovae in the past (Patel et al. 1995, 1998). Our sample of two sight lines thus may be too limited to discern the presence of a localized event. Additional F measurements are planned, expanding the sample so that about half the association will be probed. Observations of interstellar absorption from other elements having a ν-process component, such as Li and B (Woosley et al. 1990), may aid this quest. The particular enhancements from the ν-process involve the isotopes ^{7}Li and ^{11}B. The complex component structure seen toward the stars in Cep OB2 (Pan et al. 2004) essentially rules out a discriminating search based on the very weak Li I doublet at 6708 Å and on measurements of the $^{11}{\rm B}/^{10}{\rm B}$ ratio.

Data on the elemental abundance of B relative to the F abundance appear to offer the best chance to seek evidence for the ν-process in interstellar clouds. In their model of Galactic chemical evolution in the solar neighborhood, Timmes et al. (1995) suggest that ν-process synthesis of ^{11}B and F may be the controlling influence on the abundance of these light nuclides. The computed production rates depend primarily on the abundances of ^{12}C for ^{11}B and ^{20}Ne for F. These abundances in the pre-supernova's C and Ne shells, respectively, are reliably predicted. Hence, the B/F ratio from the ν-process is predictable. The calculations show that the B/F ratio is increased by a factor of about 30 when ν-process contributions are included, yielding a ratio like the solar system's for SNe II from stars with solar metallicity. Since the $^{11}{\rm B}/^{10}{\rm B}$ ratio is about 4 in diffuse interstellar clouds (Federman et al. 1996; Lambert et al. 1998), such a large enhancement for ^{11}B from the ν-process should be easily identifiable in regions affected by SNe II.

5. CONCLUDING REMARKS

We present the first interstellar fluorine measurements with *FUSE* and described the methodology to extract the F column density. The strongest F I line at 954 Å is blended with lines from H_2; a prescription for extracting information on F I from the blend was given. In the process, we determined that the line at 954 Å can be measured as long as $N(H_2)$ was less than about 3×10^{20} cm^{-2}. The inferred F/O ratio suggests that F is more depleted than O, consistent with expectations from condensation temperatures. While our goal to find a clear signature for the ν-process from F measurements was not achieved in these first observations, we offered suggestions for furthering the search. Additional F I observations are planned, and determinations of the B/F ratio offer possibly the best means for seeking evidence for the ν-process in interstellar space.

S. R. F. thanks the Department of Astronomy at the University of Texas at Austin, where much of this paper was written, for its hospitality. Observations made with the NASA/ESA *Hubble Space Telescope* were obtained from the Multiwavelength Archive at the Space Science Telescope Institute. STScI is operated by the Association of Universities for Research in Astronomy, Inc. under NASA contract NAS 5-26555. This work was supported in part by NASA grants NAG5-4957, NAG5-8961, and NAG5-10305 and grant GO-08693.03-A from the Space Telescope Science Institute to the University of Toledo. V. V. S. was funded through NASA grant NAG5-9213 to the University of Texas at El Paso.

REFERENCES

Allende Prieto, C., Lambert, D. L., & Asplund, M. 2001, ApJ, 556, L63
Anders, E., & Grevesse, N. 1989, Geochim. Cosmochim. Acta, 53, 197
Bohlin, R. C., Jenkins, E. B., Spitzer, L., Jr., York, D. G., Hill, J. K., Savage, B. D., & Snow, T. P., Jr. 1983, ApJS, 51, 277
Cartledge, S. I. B., Lauroesch, J. T., Meyer, D. M., & Sofia, U. J. 2004, ApJ, 613, 1037
Cartledge, S. I. B., Meyer, D. M., Lauroesch, J. T., & Sofia, U. J. 2001, ApJ, 562, 394
Cunha, K., Smith, V. V., Lambert, D. L., & Hinkle, K. H. 2003, AJ, 126, 1305
Danks, A. C., Federman, S. R., & Lambert, D. L. 1984, A&A, 130, 62
Diplas, A., & Savage, B. D. 1994, ApJS, 93, 211
Federman, S. R. 1982, ApJ, 257, 125
Federman, S. R., Lambert, D. L., Cardelli, J. A., & Sheffer, Y. 1996, Nature, 381, 764
Grevesse, N., & Sauval, A. J. 1998, Space Sci. Rev., 85, 161
Jorissen, A., Smith, V. V., & Lambert, D. L. 1992, A&A, 261, 164
Knauth, D. C., Federman, S. R., & Lambert, D. L. 2003, ApJ, 586, 268 (erratum, 594, 664)
Lambert, D. L., Sheffer, Y., Federman, S. R., Cardelli, J. A., Sofia, U. J., & Knauth, D. C. 1998, ApJ, 494, 614
Liu, X.-W. 1998, MNRAS, 295, 699
Lodders, K. 2003, ApJ, 591, 1220
Mowlavi, N., Jorissen, A., & Arnould, M. 1998, A&A, 334, 153
Meyer, D. M., Cardelli, J. A., & Sofia, U. J. 1997, ApJ, 490, L103
Meyer, D. M., Jura, M., & Cardelli, J. A. 1998, ApJ, 493, 222
Meynet, G., & Arnould, M. 2000, A&A, 355, 176
Morton, D. C. 2003, ApJS, 149, 205
Neufeld, D. A., Zmuidzinas, J., Schilke, P., & Phillips, T. G. 1997, ApJ, 488, L141
Pan, K., Federman, S. R., Cunha, K., Smith, V. V., & Welty, D. E. 2004, ApJS, 151, 313
Patel, N. A., Goldsmith, P. E., Snell, R. L., & Xie, T. 1995, ApJ, 447, 721
Patel, N. A., et al. 1998, ApJ, 507, 241
Savage, B. D., Cardelli, J. A., & Sofia, U. J. 1992, ApJ, 401, 706
Schectman, R. M., Federman, S. R., Beideck, D. J., & Ellis, D. G. 1993, ApJ, 406, 735
Snow, T. P., Jr., & York, D. G. 1981, ApJ, 247, L39
Timmes, F. X., Woosley, S. E., & Weaver, T. A. 1995, ApJS, 98, 617
Welty, D. E., & Hobbs, L. M. 2001, ApJS, 133, 345
Woosley, S. E., Hartmann, D. H., Hoffman, R. D., & Haxton, W. C. 1990, ApJ, 356, 272
Zhu, C., Krems, R., Dalgarno, A., & Balakrishnan, N. 2002, ApJ, 577, 795
Zmuidzinas, J., Blake, G. A., Carlstrom, J., Keene, J., & Miller, D. 1995, ApJ, 447, L125